Title	Toughness Improvement of the HAZ for Machine Structural Carbon and Low Alloy Steels (Report 4) : Effect of PWHT on the Absorbed Energy of HAZ for Medium, High Carbon Machine Structural Steels(Materials, Metallugy & Weldability)
Author(s)	Matsuda, Fukuhisa; Liu, Wu Shyuan; Magula, Vladimir
Citation	Transactions of JWRI. 1991, 20(1), p. 61-68
Version Type	VoR
URL	https://doi.org/10.18910/12349
rights	
Note	

Toughness Improvement of the HAZ for Machine Structural Carbon and Low Alloy Steels (Report 4)
—Effect of PWHT on the Absorbed Energy of HAZ for Medium, High Carbon Machine Structural Steels—

Fukuhisa MATSUDA*, Wu Shyuan LIU**, Vladimir MAGULA***

Abstract

In the previous papers[1,2], the authors have investigated the ductility of simulated HAZ using "Gleeble 1500" in continuous cooling methods and isothermal heating treatment methods during weld heat cycle in medium, high carbon steels with or without alloying element.

The improvement of toughness for higher carbon steels than 0.25%C was generally poor in continuous cooling methods, but the ductility of these steels could be fairly improved in isothermal heating treatment methods in comparison with the results of the continuous cooling methods, although the degree of improvement is depending on carbon level of steel.

Therefore, this paper has been investigated on the improvement of toughness by means of PWHT (Post Weld Heat Treatment) after the continuous cooling for medium and high carbon steels.

Main conclusions obtained are as follow:

(1) For rapid cooled HAZ to room teperature as Δ $t_{8/3}$: 12sec increasing heating temperature up to 923K in PWHT is increased the absorbed energy for each steels.

(2) For HAZ having slow continuous cooling time PWHT treatment for lower temperature decreased inversely the absorbed energy in comparison with that of non PWHT

KEY WORDS: (Heat-Affected Zone), (Post Weld Heat Treatment),(Medium, High Carbon Machine Structural Steels) (Toughness), (Improvement)

Introduction

It is well-known that medium, high carbon and low alloy steels with carbon content of 0.3 to 1.0% are often used for special purposes in the industry. Usually these steels are avoided to weld with fusion welding process because there are two disadvantages of cold cracking and poor ductility in the HAZ.

However, in the recent advance of welding process these steels are expected to be used for special construction in the industry. Therefore, the weldability of these steels is required to make clear more.

The investigation of cold crack susceptibility for these steels has been investigated clearly[3], but the improvement of HAZ ductility for these steels has not been made clear yet.

Then, in the previous papers[1,2], the authors have investigated the improvement of HAZ ductility for these steels in continuous cooling and isothermal heating treatment methods. The improvement of ductility of HAZ was made clear in isothermal heat treatment during cooling of HAZ in comparison with that of continous cooling method. However the degree of the improvement is depending on carbon level of steel and not enough as expected. Therefore, the authors wish to investigate here the improvement of ductility of HAZ in medium and high carbon plain steels by means of Post Weld Heat Treatment (PWHT) up to 923K after continuous cooling treatment with variousΔ $t_{8/3}$.

2. Experimental procedures

2.1 Steels used

Medium and high carbon steel bars of JIS S25C, S35C, S40C, S55C, SKV70 and SK5 were used as base metal. All of these are commercial steel bars whose chemical compositions are given in **Table 1.**

Table 1 Chemical composition and impact value of steels used

Steels	Chemical Composition (wt. %)										Impact Value (J)
	C	Si	Mn	P	S	Ni	Cr	Mo	N	O	
S35C	0.33	0.24	0.69	0.018	0.018	0.02	0.03	0.01	0.0056	0.004	34.1
S40C	0.39	0.25	0.70	0.026	0.028	0.02	0.12	0.01	0.0046	0.002	31.0
S55C	0.54	0.26	0.69	0.022	0.011	0.05	0.19	0.02	0.0037	0.001	12.8
SKV70	0.72	0.22	0.75	0.025	0.023	0.07	0.22	0.01	0.0096	0.002	8.5
SK5	0.89	0.24	0.29	0.022	0.020	0.04	0.12	-	0.0043	0.001	9.6

2.2 Experimental procedures

The shape and size of the simulated round bar impact specimen whose center is placed a circular notch is shown in **Fig. 1**, The dimension of the notch is according to the JIS standard charpy impact specimen.

Simulated weld thermal cycle is given by a testing machine of Gleeble 1500 which is based on resistant heating.

In this investigation thermal cycles were adopted as shown in **Fig. 2**. Time for heating from room temperature (293K) to grain boundary liquation temperature (peak temperature, T_P) is 12sec, and for holding at the T_P is 6sec. T_P for S25C, S35C, S40C, S55C, SKV70 and SK5 was given 1643, 1633, 1623, 1583, 1558 and 1548K respectively. On the cooling cycle, cooling time from 1073 to 573K (800 to 300°C, $\Delta T_{8/3}$) was changed to 4 levels of 12, 50, 71 and 195sec, and cooled to room temperature (about 293K) in

Testing temperature
: room temperature
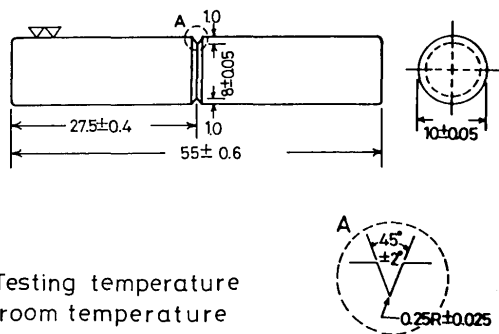
Fig. 1 Shape and size of the simulated round bar impact specimen
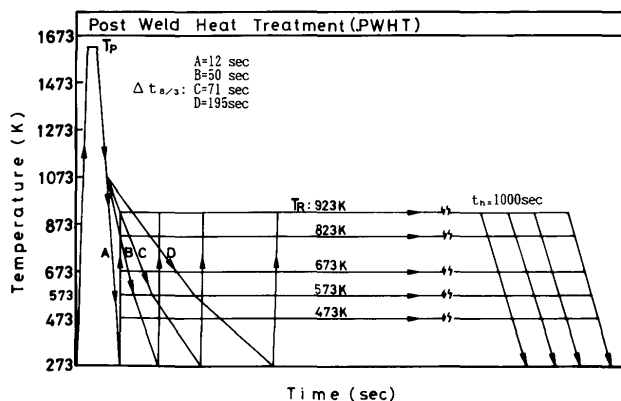
**Fig. 2** Thermal cycle for simulated toughness test as PWHT method

each cooling time cycle. For post weld heat treatment (PWHT) cycle, heating rate from 293K to each treatment temperature T_R (T_R: 473, 573, 673, 823 and 923K) was about 313K/s and after heated to each T_R the specimen was kept for treatment time (t_h: 1000sec). Further, cooling to the room teperature after the treatment was let by cooling rate of 276K/s.

After charpy impact testing the specimen was axially cut and polished for metallographic investigation. Then the metallographic microstructures were observed by optical microscope, scanning electron microscope (SEM) and transmission electron microscope (TEM; thin foil and carbon replica methods).

3. Experimental Results and Discussions

3.1 Behavior of absorbed energy

Figures 3,4,5,6 and 7 show the relationships between $\Delta t_{8/3}$ (12, 50, 71, 195sec) and absorbed energy after various PWHT for simulated HAZ of continuous cooled S35C, S40C, S55C, SKV70 and SK5 respectively. Here the value of ( ) is shown as martensite ratio after continuous cooling in each $\Delta t_{8/3}$ respectively, and the dotted line shows the absorbed energy of continuous cooling treatment without PWHT. Generally, with increasing holding temperature the absorbed energy is improved fairly. Furthermore, increasing $\Delta t_{8/3}$ shows a decrease in absorbed energy in each steel at same holding temperature. Moreover, at the
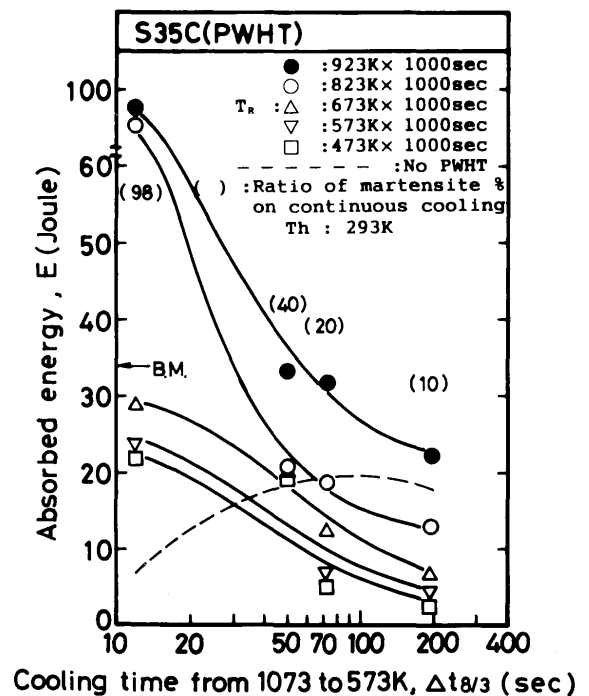
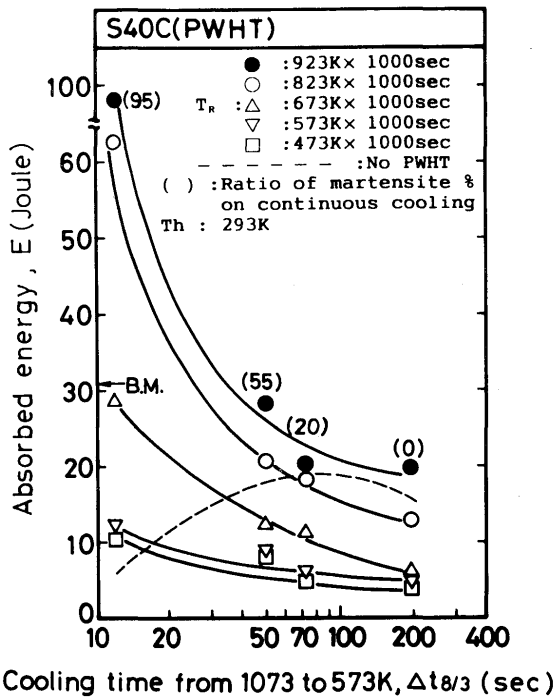**Fig. 3** The relationship between $\Delta t_{8/3}$ and absorbed energy on PWHT of S35C

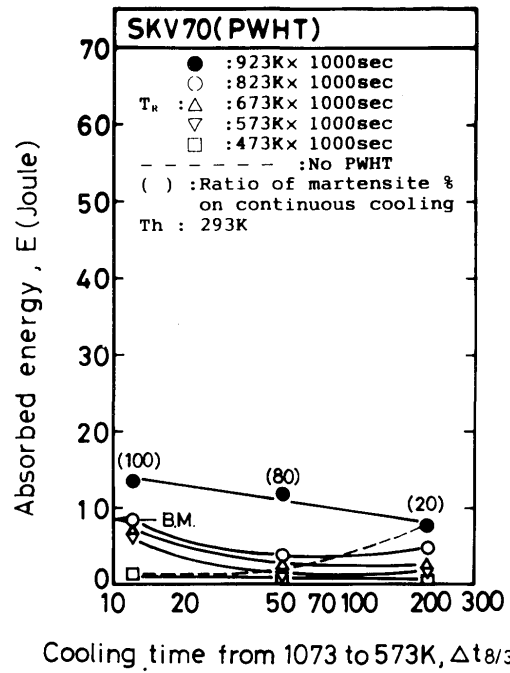**Fig. 4** The relationship between $\Delta t_{8/3}$ and absorbed energy on PWHT of S40C

Fig. 6 The relationship between $\Delta t_{8/3}$ and absorbed energy on PWHT of SKV70
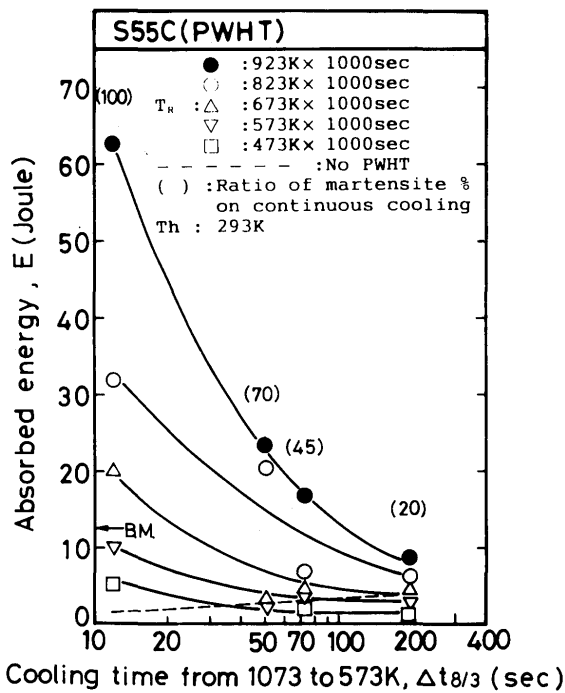

Fig. 5 The relationship between $\Delta t_{8/3}$ and absorbed energy on PWHT of S55C
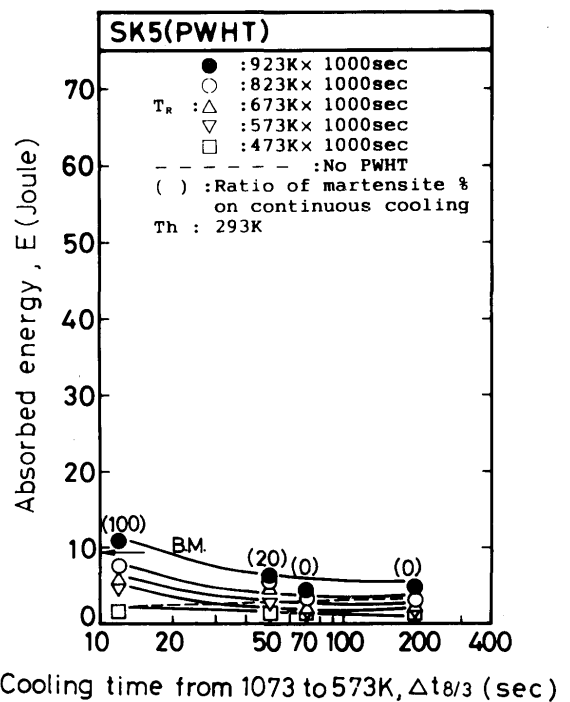

Fig. 7 The relationship between $\Delta t_{8/3}$ and absorbed energy on PWHT of SK5
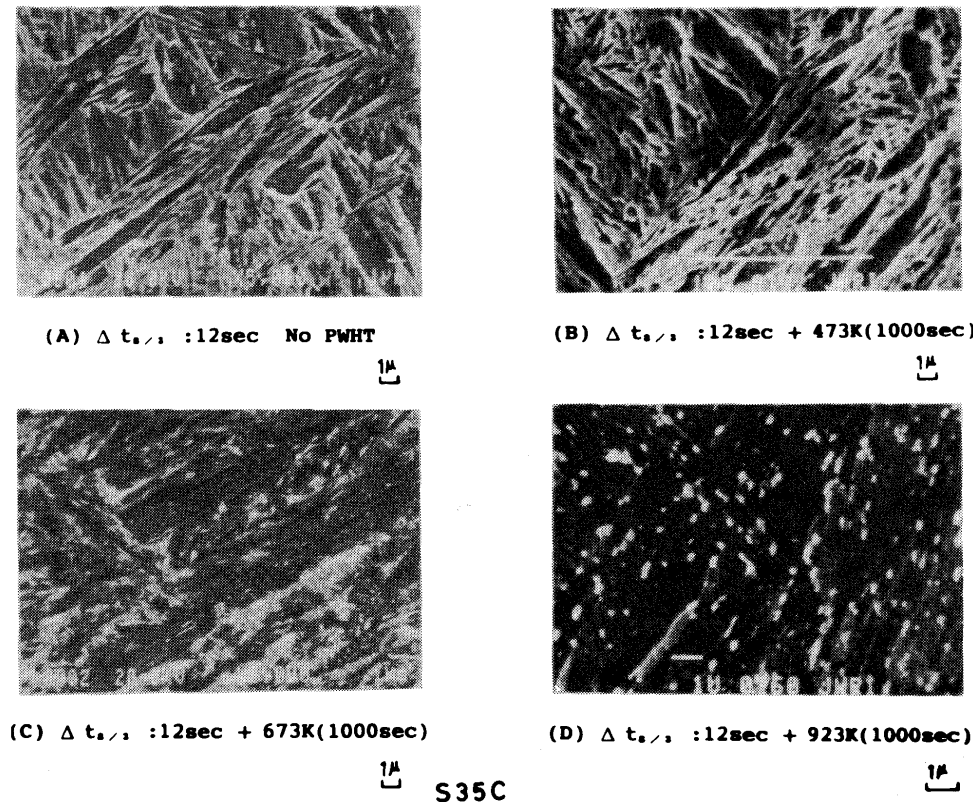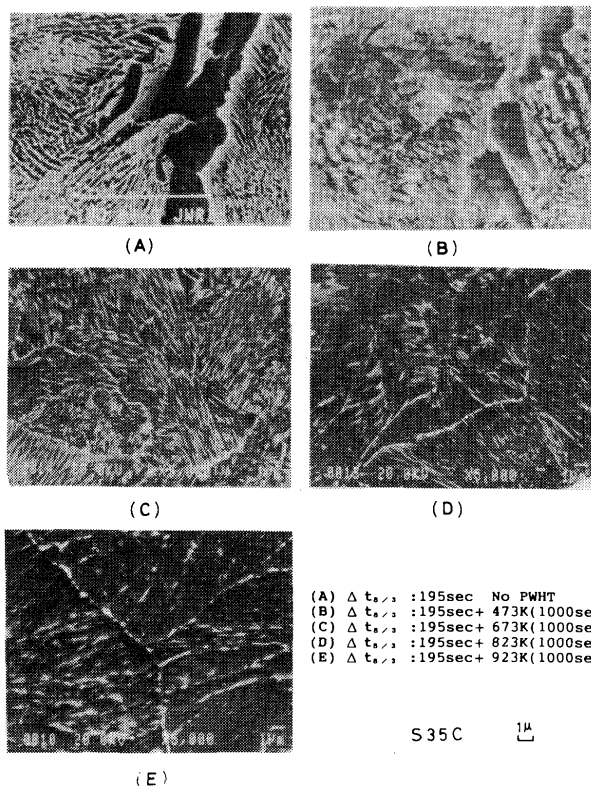
(A) Δ t₈/₃ :12sec No PWHT

(B) Δ t₈/₃ :12sec + 473K(1000sec)

(C) Δ t₈/₃ :12sec + 673K(1000sec)

(D) Δ t₈/₃ :12sec + 923K(1000sec)

S35C

Fig. 8 Optical microstructure of S35C on Δ $t_{8/3}$: 12sec
(A) Non PWHT
(B) With PWHT on 473K 1000sec
(C) With PWHT on 673K 1000sec
(D) With PWHT on 923K 1000sec

(A)

(B)

(C)

(D)

(A) Δ t₈/₃ :195sec No PWHT
(B) Δ t₈/₃ :195sec+ 473K(1000sec)
(C) Δ t₈/₃ :195sec+ 673K(1000sec)
(D) Δ t₈/₃ :195sec+ 823K(1000sec)
(E) Δ t₈/₃ :195sec+ 923K(1000sec)

(E)

S35C

shortest Δ $t_{8/3}$ (12sec) the absorbed energy are higher than the other Δ $t_{8/3}$ in each holding temperature clearly. That is to say, the structure containing higher amounts of martensite is easy to recover the ductility by PWHT, even though initial ductility is very low due to martensite.

From the results of Figs. 3 to 7 it is considered that fair improvement of the ductility on the HAZ is expected only for shorter cooling time of Δ $t_{8/3}$ after higer temperature in PWHT.

As a result, in comparison with the absorbed energy of continuous cooling treatment without PWHT, the ductility after lower temperature treatment for slow continuous cooled HAZ is deteriorated, especially when the holding temperature is lower than 773K in each steel for 195sec of Δ $t_{8/3}$. It is obvious that low temperature temper embrittlement would occur due to precipitation of carbide in ferrite as discuss in the section 3.3.

Fig. 9 Optical microstructure of S35C on Δ $t_{8/3}$: 195sec of SEM
(A) Non PWHT
(B) With PWHT on 473K 1000sec
(C) With PWHT on 673K 1000sec
(D) With PWHT on 823K 1000sec
(E) With PWHT on 923K 1000sec

3.2 Microstructural investigations

Figures. 8(A), (B), (C) and **(D)** show the microstructural change of S35C with SEM for non, 473, 673 and 923K PWHT with 1000sec after Δ $t_{8/3}$: 12sec continuous cooling respectively. Fig. 8(A) shows the microstructure of almost plate-like martensite, Fig. 8(B) shows almost thhe martensite structure without precipitated, but in Fig. 8(C) there is a part of spheroidal carbide which was resolved from martensite. Moreover, Fig. 8(D) shows sorbitic microstructure with spheroidal carbide which was precipitated and resolved in ferrite matrix.

Therefore, in case of fast continuous cooling the absorbed energy is increased with an increase of PWHT temperature by changing the structure from martensite to tempered martensite and sorbite.

Furthermore, increasing PWHT temperature from 673 to 823K the toughness is abruptly increased by the changing of linear to spheroidal shaped carbides.

Figures 9(A), (B), (C), (D) and (E) show the microstructural change of S35C with SEM for non, 473, 673, 823 and 923K PWHT with 1000sec after Δ $t_{8/3}$: 195sec continu-

ous cooling respectively.

Fig. 9(A) shows the lamellar pearlite inside the prior austenite grain and the proeutectoid ferrite structures precipitated in the grain boundary, Fig. 9(B) shows almost the same structure as in Fig. 9(A), although 473K, 1000sec PWHT treatment was performed. However Fig. 9(C) shows that a small part of pearlite colony was formed to spheroidal carbide, therefore, for higher temperature than this treatment the cementite is resolved to spheroidal carbide gradually. Furthermore, in Fig. 9(D) the spheroidal carbide was formed more than in Fig. 9(C). Finally in Fig. 9(E) spheroid of carbide is obviously adavanced and spheroidal carbides are intermittently observed all over the structure. However the improvement of toughness is not so advanced as shown in Fig. 3.

Figures 10(A), (B), (C), (D) shows the fractographies of fractured specimens in the above conditions except 823K 1000sec treated specimen. In these photograpies there are shown almost the same transgranular fracture (cleavage fracture), and the unit of facet of the fracture was almost the same size as a pearlite colony as measured, Therefore, it is considered that the transgranular fracture was started
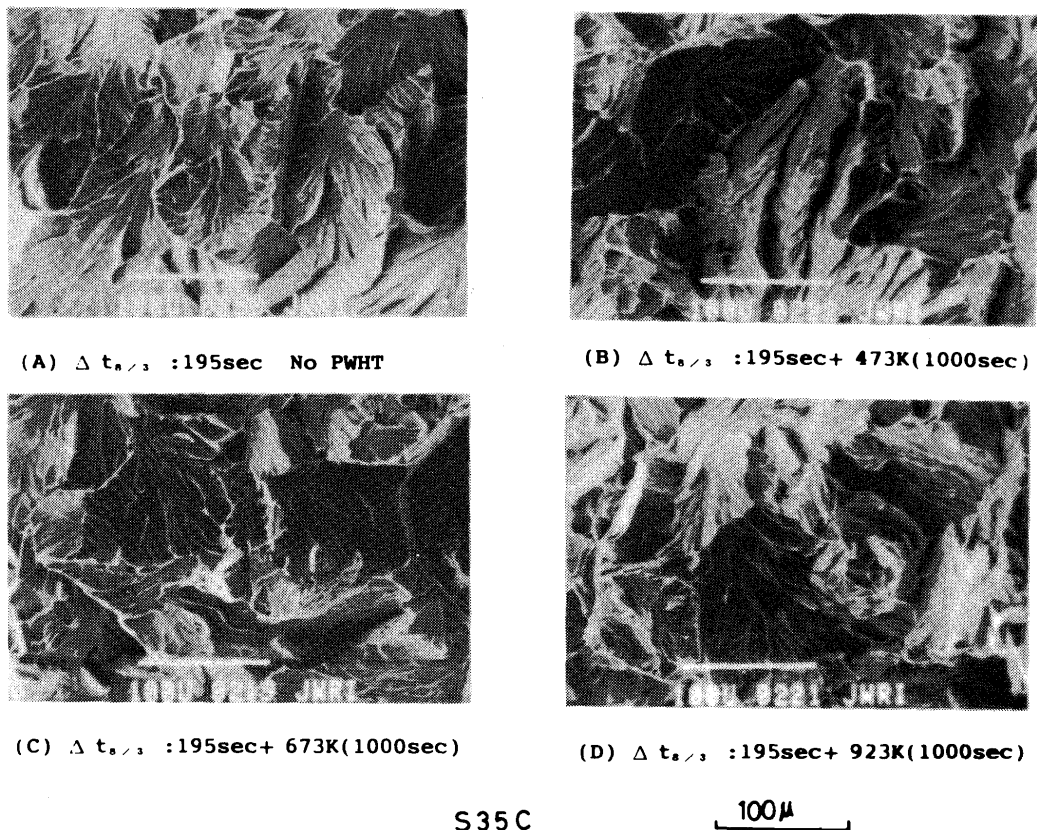

(A) Δ $t_{8/3}$:195sec   No PWHT

(B) Δ $t_{8/3}$:195sec+ 473K(1000sec)

(C) Δ $t_{8/3}$:195sec+ 673K(1000sec)

(D) Δ $t_{8/3}$:195sec+ 923K(1000sec)

S35C   100μ

Fig. 10 Fracture surface of S35C on Δ $t_{8/3}$: 195sec of SEM
  (A) Non PWHT
  (B) With PWHT on 473K 1000sec
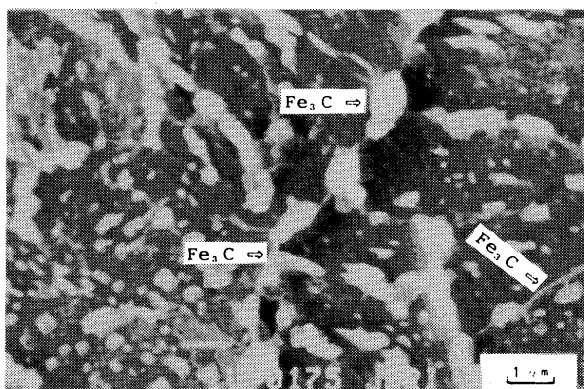 (C) With PWHT on 673K 1000sec
  (D) With PWHT on 923K 1000sec

Fig. 11 Fracture surface of S35C on △ t₈/₃: 195sec with PWHT
on 923K 1000sec by SEM

from the boundary between the pearlite colonies.

Again in **Fig. 11** the enlarged photograph of carbide in the pearlite colony of 923K 1000sec treated specimen after Δ t₈/₃: 195sec continuous cooling. In this photograph, film-like shaped carbides (Fe₃C cementite in diffraction pattern) are still existing between spheroidal carbides along the boundary of pearlite colony. It is considered that, because of the effect of easier stress concentration and higher dislocation density due to this carbide, the impact fracture is easier to start from these thin film of carbide.

3.3 Discussion of deterioration of toughness

In Figures 3 through 7, there are shown that, when the lower temperature treatment of PWHT after continuous cooling in slow Δ t₈/₃ is performed, the absorbed energy of all steels is lower than that without PWHT. Therefore in this section, the authors have investigated the distribution of dislocation and precipitating behavior in the boundary proeutectoid ferrite.

Figures 12(A), (B), (C), (D) and (E) show the distributions of dislocation in proeutectoid ferrite of grain boundary of prior austenite under non PWHT, 473, 573, 673 and 823K with 1000sec treatment after Δ t₈/₃: 195sec continuous cooling respectively. Generally, the density of dislocation gradually decreases with increasing treatment temperature after the maximun at 473K. This is considered that the density of dislocation in ferrite affects a decrease in the ductility due to precipitation of fine carbide or nitride. However in the type of aging embrittlement precipitates is usually difficult to be detected even in TEM because of too fine particles.

Therefore **Fig. 13** shows the relationship between aging time of 473 K PWHT treatment and hardness in boundary proeutectoid ferrite after 195sec continuous cooling for S35C. Generally, increasing aging time shows an increase in hardness up to about 4hrs, and a decrease again thereafter. That is to say, the resolved impurties would be
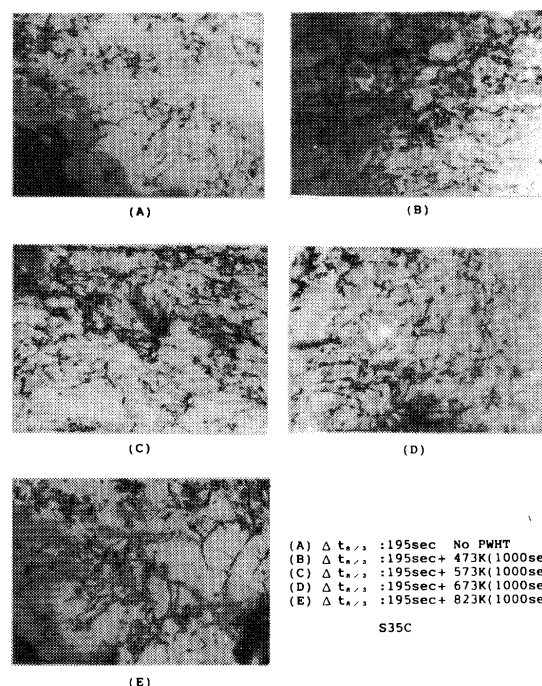

(A) △ t₈/₃ :195sec No PWHT
(B) △ t₈/₃ :195sec+ 473K(1000sec)
(C) △ t₈/₃ :195sec+ 573K(1000sec)
(D) △ t₈/₃ :195sec+ 673K(1000sec)
(E) △ t₈/₃ :195sec+ 823K(1000sec)

S35C

Fig. 12 Dislocation's distribution on boundary ferrite on △ t₈/₃: 195sec with various PWHT by TEM
(A) Non PWHT
(B) With PWHT on 473K 1000sec
(C) With PWHT on 573K 1000sec
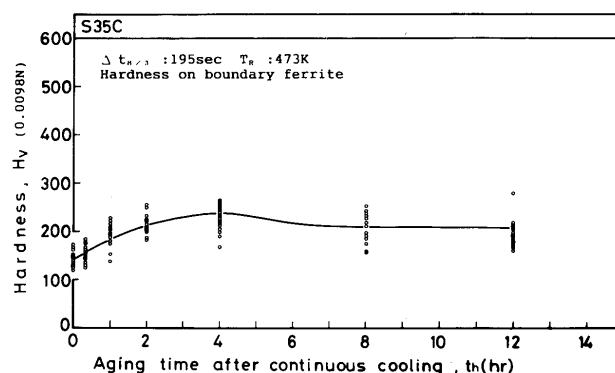(D) With PWHT on 673K 1000sec
(E) With PWHT on 823K 1000sec

Fig. 13 Hardness of boundary ferrite on △ t₈/₃: 195sec with 473K holding temperature and various aging time

precipitated into boundary ferrite as coherent situation to matrix up to about 4hrs of aging time. However, more than about 4hrs of aging time the impurities would be precipitated into ferrite as incoherent situation to matrix, then the hardness would be decreased gradually.

Figures 14(A), (B) and (C) show the impurities precipitated into boundary ferrite after 473K 8hrs PWHT by thin foil method of TEM. Fig. 14(A) shows the photo in the bright field and Fig. 14(B) the dark field for impurities in the boundary proeutectoid ferrite. Fig. 14(C)
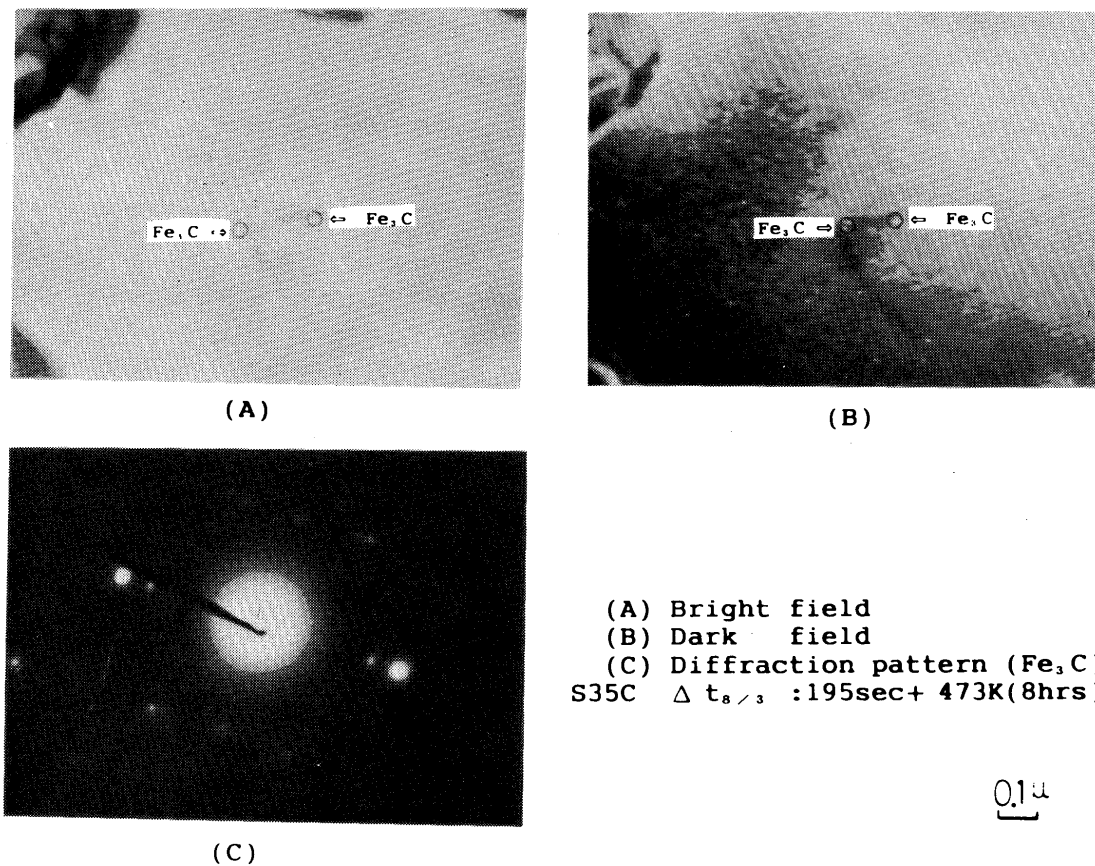
(A)

(B)

(C)

(A) Bright field
(B) Dark   field
(C) Diffraction pattern (Fe₃C)
S35C Δ t₈/₃ :195sec+ 473K(8hrs)

$\underset{\longmapsto}{0.1\mu}$

Fig. 14 Precipitated carbides on boundary ferrite on Δ $t_{8/3}$: 195sec with 473K 8hrs PWHT
(A) Bright field
(B) Dark field
(C) Diffraction pattern

shows the diffraction pattern of the impurity which is designated as Fe_3C carbide. Furthermore, these carbides were not detected to precipitate into the ferrite in the case of 4hrs aging time.

Therefore, it is considered that the deterioration of toughness was caused by the pre-stage or fine precipitation of carbide into ferrite during lower temperature treatment.

4. Conclusion

This paper has been investigated the effect of PWHT on improvement of the toughness of HAZ of medium and high carbon steels (0.24~0.89% C) after simulated continuous cooling treatments. Thermal cycles were given by Gleeble 1500 for simulated HAZ. The continuous cooling times of Δ $t_{8/3}$ were given as 12, 50, 71 and 195sec, and the PWHT conditions after continuous cooling were given by 5 levels of holding temperature as 473, 573, 673, 823 and 923K with holding time of 1000sec for each steel.

Main conclusions obtained are as follows

(1) The structure in the simulated HAZ in which amount of martensite is higher due to rapid cooling is gradually improved in absobed energy by increasing of PWHT temperature from 473 to 923K.
However an increase of absorbed energy is obvious in temperature between 673 and 823K.

(2) The structure in which proeutectoid ferrite and pearlite governs due to slow cooling is deteriorated in absorbed energy by PWHT of lower temperature as 473 to 673K. The deterioration of absorbed energy is the most at 473K, and gradually is improved with increasing temperature. Furthermore the absorbed energy of the structure exceeds to that of non PWHT HAZ by 923K treatment.

(3) By PWHT of 923K the improvement of absorbed energy is better in rapid cooling HAZ and lesser in slow cooling HAZ. The reason why the latter is lesser is considered to be difficulty of spheroid of carbide.

(4) The deterioration of absorbed energy in lower temperature PWHT in slow cooling HAZ is considered to be caused by the hardening due to carbide precipitation into proeutectoid ferrite. Precipitation of carbides by aging in 473K are observed into the ferrite by TEM.

(5) From the standpoint of toughness of HAZ in actual welding operation the authors can recommend for the preheating and PWHT in welding of medium and high carbon steel as,

(a) Lower preheating and higher PWHT temperature is the most recommendatory for improving toughness, although lower preating is susceptible to quench cracking due to high hardenability.

(b) Slow cooling and lower PWHT temperature is the most unrecommendatory because of deterioration of toughness, although it is better to avoid quench cracking. Futhermore slow cooling and higher PWHT increases toughness, but not so enough as expected. It means that ductility of the HAZ with higher preheating and low temperature reheating by multipass layer welding are not always advantages for ductility improvement.

(c) Selection of the optimum preheating and PWHT temperature should be considered for the HAZ from the standpoints of avoidance of quench cracking and improvement of ductility.

Reference

1) F. Matsuda et al.: Trans, JWRI, 18–2 (1989). p 79–84

2) F. Matsuda et al.: Trans, JWRI, 18–2 (1989). p 85–90

3) F. Matsuda et al.: Trans, JWRI, 15–2 (1986). p 135–141